Langmuir

Article

pubs.acs.org/Langmuir

A Molecular and Thermodynamic View of the Assembly of Gold Nanoparticles in Nematic Liquid Crystal

Jonathan Milette,[†] Violeta Toader,[†] Ezequiel R. Soulé,[‡] R. Bruce Lennox,[†] Alejandro D. Rey,*[,§] and Linda Reven*[,†]

[†]Centre for Self-assembled Chemical Structures, Department of Chemistry, McGill University, 801 Sherbrooke St. W., Montreal, QC H4A 3B7, Canada

[‡]Institute of Materials Science and Technology (INTEMA), University of Mar del Plata and National Research Council (CONICET), J. B. Justo 4302, 7600 Mar del Plata, Argentina

[§]Department of Chemical Engineering, McGill University, 3610 University Street, Montreal, QC H3A 2B2, Canada

Supporting Information

ABSTRACT: The molecular interactions driving the assembly of gold nanoparticles (AuNPs) in a nematic liquid crystal (LC) are directly detected by nuclear magnetic resonance (NMR) spectroscopy and thermodynamically analyzed. The orientational orders of the selectively deuterated LC matrix and AuNP ligands, each separately followed by variable temperature ^{2}H NMR as a function of particle concentration, were observed to be strongly correlated. The mechanism of the reversible formation of long-range, quasi-periodic nanoparticle structures is attributed to the coupling of the AuNP ligands to the LC matrix, inducing an isotropic−nematic biphasic state. Experimentally validated thermodynamic modeling shows that, in contrast to colloidal nematics that are dominated by elastic forces, nematic dispersions of nanoparticles self-organize through a subtle balance of entropic forces and excluded volume, interface-mediated mesogen and nanoparticle molecular interactions, and couplings between conserved and nonconserved order parameters. Fine-tuning of these interactions through ligand and mesogen chemistry, together with mesoscale modeling, provides a route for materials innovations by merging structured fluid physics and nanoscience.

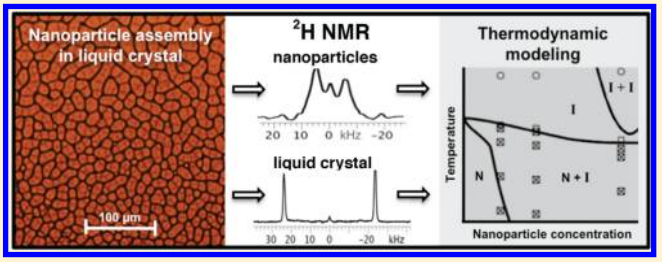

INTRODUCTION

Many efforts are underway to develop liquid crystalline nanocomposites with the goals of spatially organizing the nanomaterials and/or enhancing the properties of both the nanomaterial and its liquid crystal (LC) host.[1,2] In addition to using nanoparticles (NPs) as a dopant to improve the electro-optical performance of LC-based devices, the LC-mediated assembly of NPs to form new tunable metamaterials for electronic, photonic, and optical applications is a highly sought-after goal.[3] The synthetic and theoretical aspects of this research field are still at an early stage, however, with methods to reproducibly produce homogeneous NP dispersions in LCs proving to be very challenging to develop. Colloidal nematics, where micrometer-size particles are dispersed in the nematic phase of a LC, have been intensively studied over the past 20 years.[4,5] When the particle size is reduced to the nanometer scale, the effect on the LC defect structure and the interparticle interactions are expected to drastically change.[6] In colloidal nematics, the interparticle interactions are due to long-range orientational distortion of the LC about the colloid. As the particle size decreases, these LC-mediated particle interactions are predicted to diminish, offering the possibility of forming well-defined structures through reversible association combined with tuning of the anchoring energies.[7]

We have recently developed a method to produce long-range, quasi-periodic, and reversible nanoparticle assemblies by taking advantage of the LC phase transitions.[8] The formation of these ordered structures, instead of a simple phase separation, requires high miscibility of the NPs in the LC solvents, achieved through fine-tuning of the capping ligand shell.[9] Gold nanoparticles (AuNPs) with a mixed monolayer of hexanethiol and the mesogenic ligand 4′-(12-mercaptododecyloxy)-biphenyl-4-carbonitrile [$CBO(CH_2)_{12}SH$] can be dispersed in isotropic 4′-pentyl-4-cyanobiphenyl (5CB) at concentrations exceeding 50 wt % Au (volume fraction, ϕ = 0.35). At the clearing point temperature of 5CB (T_{N-I}), AuNP networks of branches and circular domains are formed by enrichment of the NPs at the nematic−isotropic liquid interfaces. The dimensions, topology, and accompanying LC defect structure of the networks are controlled via the particle concentration, cooling rate, and film thickness. As discussed previously,[8] these AuNP assemblies differ from the cellular networks formed by polymer colloids[10] in terms of the topologies, mechanical properties, LC textures, and the role of impurities. The AuNPs functionalized

Received: October 22, 2012
Revised: December 22, 2012
Published: January 7, 2013

   dx.doi.org/10.1021/la304189n | *Langmuir* 2013, 29, 1258−1263

with mesogenic ligands present an ideal model system to study the LC–NP interactions at the molecular level by nuclear magnetic resonance (NMR) spectroscopy. Through isotopic labeling, the dynamics and order parameters of the ligands and host LC of AuNP dispersions can be selectively followed by variable temperature wide-line ^{2}H NMR as a function of particle concentration. We have combined this experimental approach with thermodynamic modeling to understand the mechanism of the assembly of AuNPs via the isotropic–nematic phase transition.

MATERIALS AND METHODS

Materials. The preparation of the gold nanoparticles was described previously.[9] 4′-[(12-mercaptododecyl)oxy]biphenyl-3′,5′-d_2-4-carbonitrile (CBO$(CH_2)_{12}$SH-d_2) was synthesized following a procedure that uses a deuterium-labeled 4-bromo-4′-hydroxy-biphenyl-3′,5′-d_2 as a starting material. 4-Cyano-4′-pentyl-d_2-1,1′-biphenyl (5CB-d_2) was synthesized starting from 4-bromobenzene using a four-step procedure as outlined in the Supporting Information.

The AuNPs–LC dispersions were prepared by mixing the AuNPs and LC in the NMR tube using dichloromethane as cosolvent. The mixture was sonicated for 5 min, and the solvent was evaporated under a stream of Ar(g) overnight at 40 °C under constant mixing. The residual solvent was removed under vacuum at 40 °C until no trace was detected by liquid-state NMR.

Solid-State NMR. The solid-state 61.4 MHz (^{2}H) NMR were collected on a Varian 400 NMR spectrometer with a 10 mm T3 wide line probe. A solid-echo pulse sequence was used with 5.1 μs ($\sim\pi/2$) pulse, recycling delay of 0.1 s (5CB-d_2) and 1.0 s (deuterated AuNPs), spectral width of 1250 kHz, and no ^{1}H decoupling. The samples were contained in short tubes such that they were entirely confined within the probe coil. The sample was kept in the NMR spectrometer at 38 °C (5CB isotropic phase) for 30 min before and between temperature cycling (one cycle = isotropic–crystalline–isotropic). The samples were kept for 10 min at each experimental temperature before acquiring data. No change in spectrum appearance (intensity, splitting, and shape) was observed after the 10 min. The appearance of the dispersions remained the same before and after the NMR experiments with no visible bulk phase separation.

RESULTS AND DISCUSSION

Wide-Line ^{2}H NMR Spectroscopy. *CBO$(CH_2)_{12}$SH-d_2 Ligand.* The variable temperature ^{2}H NMR spectra of CBO$(CH_2)_{12}$SH-d_2 alone, dissolved in 5CB, and bound to AuNP are presented in Figure 1. The ^{2}H NMR signal of the LC ligand in the crystalline phase or attached to AuNPs in the absence of solvent were not detected due to very long spin–lattice relaxation times.[11] The dry AuNPs functionalized with CBO$(CH_2)_{12}$SH-d_2 (AuNP-d_2) were not heated above 50 °C to avoid possible decomposition. The absence of a ^{2}H NMR signal indicates that the motion of the rings is highly restricted even when the ligand is attached to the NP surface where the surface curvature will create free volume. A high surface curvature combined with a short, bulky ligand was shown by ^{2}H NMR to greatly enhance the mobility of the molecules bound to 1.8 nm diameter AuNPs as compared to the unbound molecules.[12] In the case of the mesogenic ligands, dense packing of the cyanobiphenyl groups can be achieved through intercalation of groups between neighboring particles as observed for alkylthiol-functionalized AuNPs. Goodby and co-workers presented a model for the condensed phase of 2 nm AuNPs decorated with CBO$(CH_2)_n$SH ligands where efficient packing is achieved via interparticle π–π stacking of the cyanobiphenyl groups.[13]

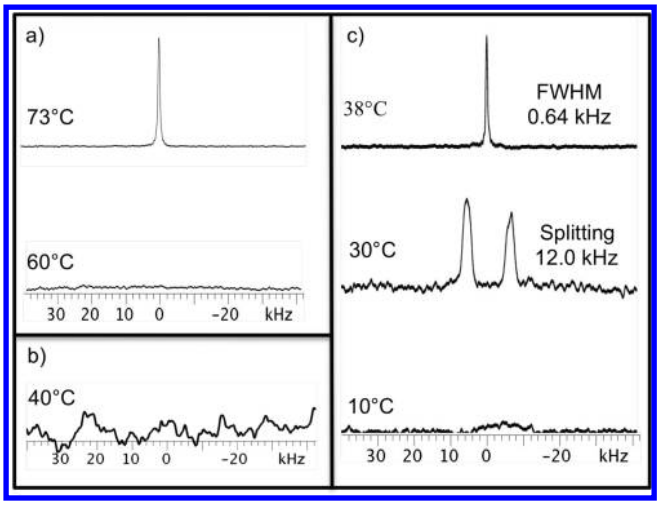

Figure 1. ^{2}H NMR of SH$(CH_2)_{12}$OCB-d_2 ligand (a) alone, (b) bound to AuNPs, and (c) in 5CB LC at 5 wt % Au.

Upon heating, no ^{2}H doublet characteristic of the nematic phase was observed for CBO$(CH_2)_{12}$SH-d_2 due to the very narrow nematic temperature range. Polarizing optical microscopy (POM) of CBO$(CH_2)_{12}$SH-d_2 showed a nematic phase with cooling between 70.7 and 70.3 °C, very similar to the data reported by Kumar.[14] When CBO$(CH_2)_{12}$SH-d_2 is dissolved in nematic 5CB, a doublet appears that collapses to a single peak in the isotropic phase of 5CB. The size of the splitting, 12 kHz, is very close to the literature value for the ring deuterons in perdeuterated 4-pentoxy-4′-cyanobiphenyl (5OCB).[15]

AuNPs Capped with CBO$(CH_2)_{12}$SH-d_2 in 5CB. The ^{2}H NMR spectra of dispersions of AuNPs capped with a monolayer of CBO$(CH_2)_{12}$SH-d_2 in 5CB are presented in Figure 2. The dispersions for the ^{2}H NMR studies were all prepared in the same way. AuNPs with increasing amounts of 5CB were prepared to make composites with decreasing volume fractions of ϕ = 0.70, 0.35, 0.14, and 0.07 (corresponding to 75, 50, 25, and 13 wt % Au) and a constant quantity of labeled material. Before each run, the dispersions were carefully homogenized by *in vacuo* mixing with a magnetic bar at 40 °C overnight and kept in the NMR spectrometer at 38 °C for 30 min. The samples were prepared in this manner to facilitate the comparison between different AuNPs and to correlate the order parameters of the LC matrix with those of the AuNP ligands. For all of the dispersions studied, it is important to recognize that there may be undetected ^{2}H NMR signal intensity from a population of immobile ligands with long relaxation times as observed for crystalline CBO-$(CH_2)_{12}$SH-d_2 and the dry AuNPs. A study of the miscibility of AuNPs capped with a monolayer of mesogenic ligands CBO$(CH_2)_n$SH (n = 8, 12, 16) showed that only the NPs capped with the n = 12 ligand partially disperse in 5CB.[9] Polarized optical microscopy (POM) images reveal that these AuNPs form a weak network upon cooling to the nematic phase.[8]

At the highest NP concentration, ϕ = 0.70 (75 wt % Au), the ^{2}H NMR spectrum of the AuNPs, capped with CBO-$(CH_2)_{12}$SH-d_2 and dispersed in isotropic 5CB, consists of a broad signal with a line width on the order of the quadrupolar splitting of CBO$(CH_2)_{12}$SH-d_2 (Figure 2j). As the particle concentration is lowered, a narrow singlet, assigned to AuNPs that are fully dispersed in 5CB, appears superimposed on the broad 12 kHz component assigned to aggregate AuNPs (Figure

dx.doi.org/10.1021/la304189n | *Langmuir* 2013, 29, 1258–1263

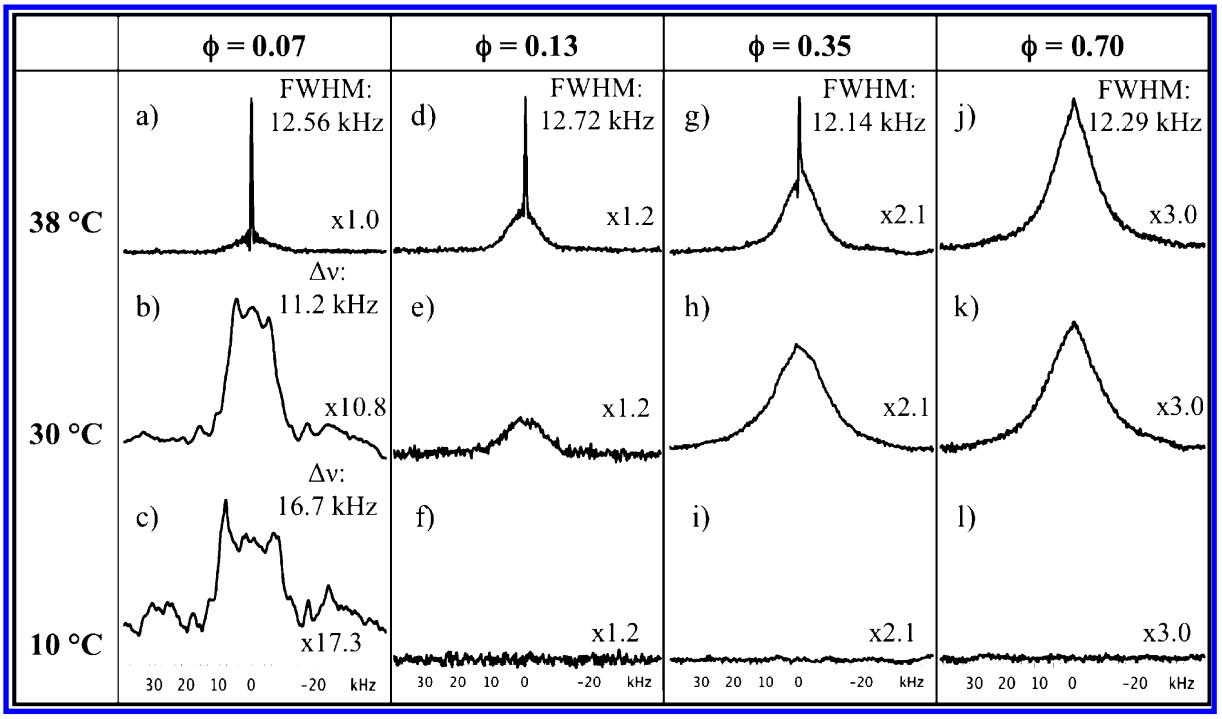

Figure 2. ^{2}H NMR spectra of AuNP capped with 100% deuterated CBO$(CH_2)_{12}$SH and dispersed in 5CB liquid crystal (upper insets for a, d, g, j = full width at half-maximum (fwhm) of the broad component and b, c = splitting of doublet ($\Delta\nu$); lower insets = intensity relative to spectrum a).

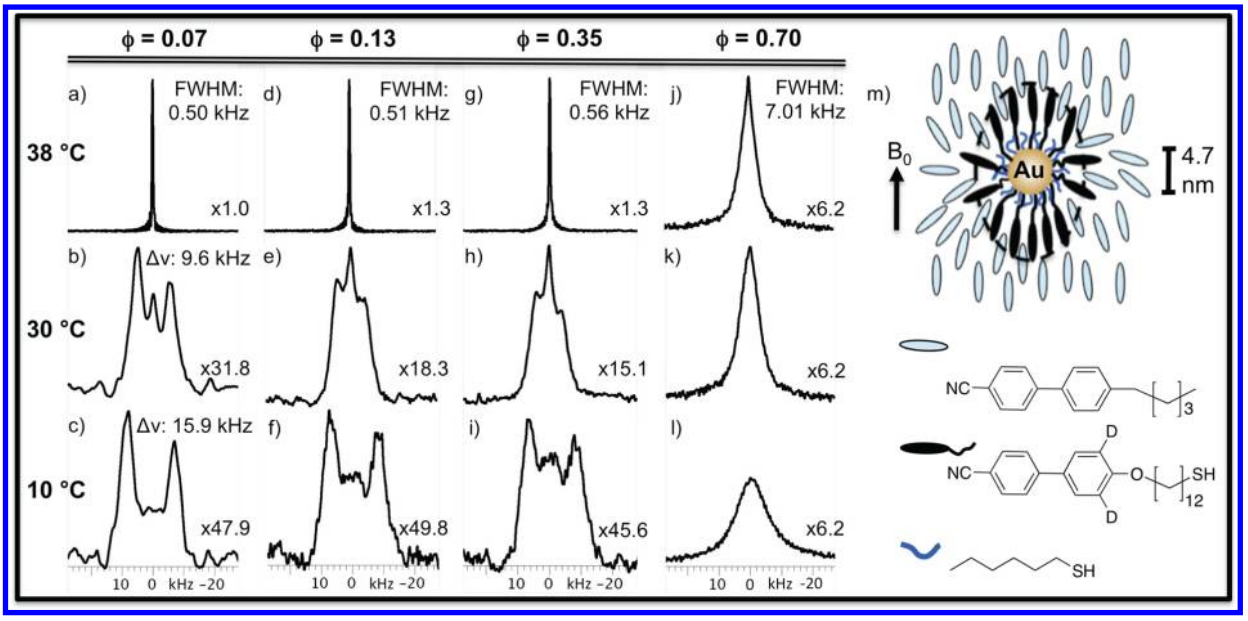

Figure 3. Left: ^{2}H NMR of AuNPs capped with 49% CBO$(CH_2)_{12}$SH-d_2 and 51% hexanethiol and dispersed in 5CB (upper insets for a, d, g, j = full width at half-maximum (fwhm) and b, c = splitting of doublet ($\Delta\nu$); lower insets = intensity relative to spectrum a). Right: schematic of a tactoidal gold nanoparticle based on ref 13 (molecular structures of 5CB (light blue), CBO$(CH_2)_{12}$SH-d_2 (black), and hexanethiol (dark blue)).

2g). The narrow peak vanishes when the host 5CB is cooled to the nematic phase, leaving the broad component. At the lowest particle concentration, a doublet signal appears in the nematic phase, superimposed on a broad singlet. The appearance of the doublet, with the same quadrupolar splitting as the ligand dissolved in 5CB, indicates that some of the ligands are aligned with the magnetic field (Figure 2b). The ^{2}H NMR line shapes of all the dispersions were found to be completely reproducible by additional temperature cycles.

AuNPs Capped with 1:1 Hexanethiol and CBO$(CH_2)_{12}$SH-d_2 in 5CB. The ^{2}H NMR spectra of dispersions of AuNPs capped with 1:1 hexanethiol and CBO$(CH_2)_{12}$SH-d_2 in 5CB are given in Figure 3. At the highest concentration, ϕ = 0.70, where no isotopic−nematic phase transition is detected by differential scanning calorimetry (DSC) (Supporting Information, Figure S1), the AuNP peak in isotropic 5CB is broad. For the ϕ = 0.35 dispersion at 38 °C (Figure 3g), a narrow singlet appears, assigned to AuNPs that are fully dispersed in isotropic 5CB even at this high particle concentration. POM images of

dx.doi.org/10.1021/la304189n | *Langmuir* 2013, 29, 1258−1263

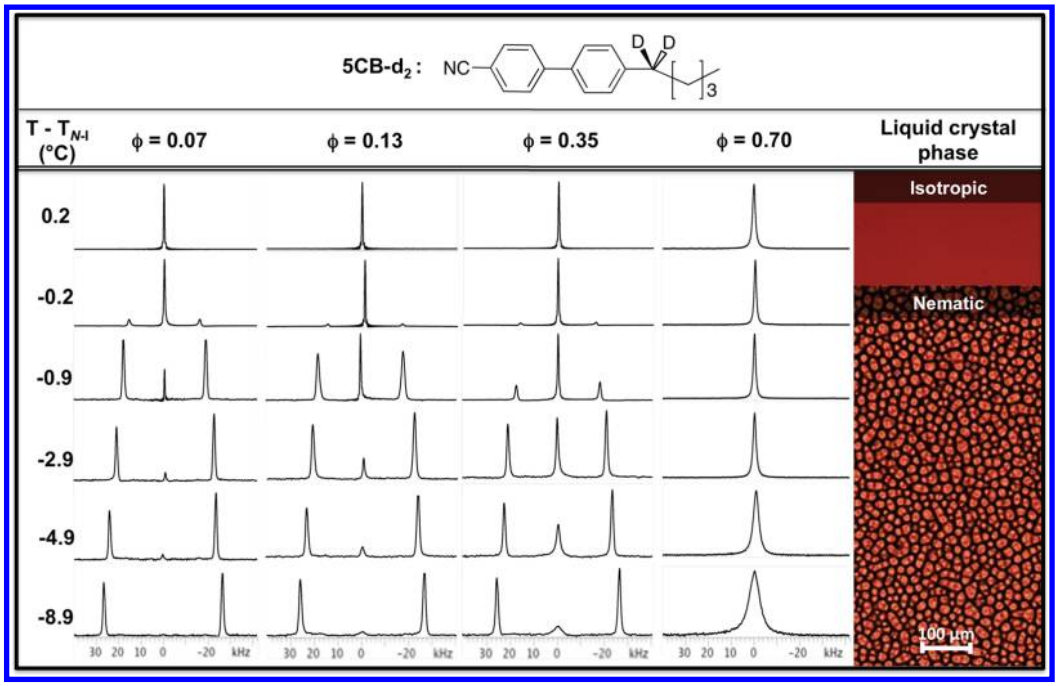

Figure 4. Left: ^{2}H NMR of AuNPs capped with a 1:1 hexanethiol and $CBO(CH_2)_{12}SH$, and dispersed in 5CB-d_2 liquid crystal as a function of particle concentration and temperature. Top: molecular structure of 5CB-d_2. Right: polarizing optical microscopy images of a $\varphi = 0.35$ dispersion of AuNPs between untreated glass slides in the isotropic and nematic phases.

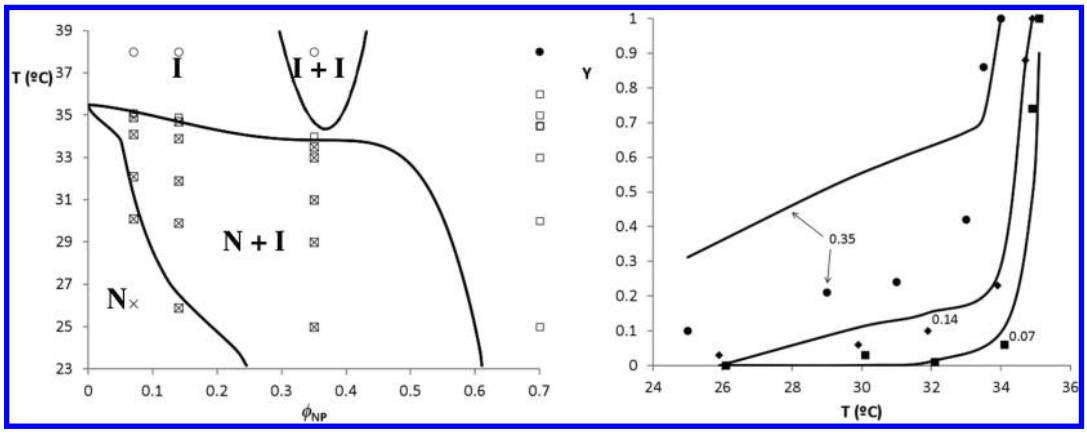

Figure 5. Left: phase diagram of AuNPs capped with 49% $CBO(CH_2)_{12}SH$ and 51% hexanethiol and dispersed in 5CB. Full lines indicate the model results, and points are results from NMR as follows: open circles correspond to sharp singlet and full circle to broad peaks in the ^{2}H NMR spectra of AuNP-d_2; open squares correspond to isotropic (singlet), crosses to nematic (doublet), and crossed squares to the coexistence in the ^{2}H NMR spectra of 5CB-d_2. Right: fraction of isotropic phase (Y) calculated from the model (full lines) and the experimental NMR data (points) as a function of temperature at $\phi = 0.07$ (bottom line and squares), $\phi = 0.14$ (middle line and diamonds), and $\phi = 0.35$ (top line and circles).

dispersions with such ^{2}H NMR spectra show either clear red liquids with no visible agglomerates or, in the case of the more concentrated samples (>13 wt % Au), agglomerates that dissipate close to T_{N-I}.[8] Below T_{N-I}, the narrow singlet spectrum of the mixed monolayer AuNPs transforms into a doublet signal superimposed on a broad singlet. The appearance of the doublet, with the same quadrupolar splitting as the ligand dissolved in nematic 5CB (Figure 1), indicates that some of the ligands are aligned with the magnetic field, in agreement with the tactoidal model proposed by Goodby,[13] shown in Figure 3. Comparison with the spectra of AuNPs capped with a monolayer of $CBO(CH_2)_{12}SH$-d_2 (Figure 2), which form only a weak network,[8] demonstrates the greatly enhanced mobility of the cyanobiphenyl groups due to the free volume created within the ligand shell by the hexanethiol spacer groups. The correlation of the doublet with the disappearance of the broad component in the isotropic phase, assigned to agglomerated AuNPs, shows that the AuNPs must be fully dispersed in the isotropic phase of the host LC in order for the ligands to align in the nematic phase.

^{2}H NMR of the Host LC: 4-Cyano-4′-pentyl-d_2-1,1′-biphenyl (5CB-d_2). The effect of the AuNPs capped with a 1:1 hexanethiol and $CBO(CH_2)_{12}SH$ on the orientational order of the LC matrix is presented in Figure 4. We first note that for the highest AuNP concentration, $\phi = 0.70$ (75 wt % Au), the isotropic-to-nematic phase transition, as indicated by the appearance of a doublet, is not detected and no nematic order evolves, also confirmed by DSC (Figure S1). Below T_{N-I} for AuNP concentrations of $\phi \leq 0.35$, the host LC is sharply partitioned into isotropic liquid and aligned nematic as

dx.doi.org/10.1021/la304189n | *Langmuir* 2013, 29, 1258−1263

indicated by the superposition of a narrow singlet peak and a full splitting doublet. The most important observation for the NMR data is that the trends in the relative intensities of the nematic and isotropic peaks of the LC matrix with temperature and NP concentration are qualitatively highly correlated with those of the doublet and singlet assigned to aligned and disordered AuNP ligands, respectively. Despite a significant fraction of isotropic 5CB detected by NMR for high AuNP concentrations, no isotropic liquid is detected by POM in the light regions of the host LC between the dark branches (Figure S4), and we conclude that the isotropic liquid is located in the dark regions that consist of AuNP enriched 5CB (network branches).

THERMODYNAMIC MODELING

The presence of the singlet and doublet peaks in the ^{2}H NMR spectra enabled us to construct a phase diagram for the AuNPs−LC composite as a function of particle concentration and temperature (Figure 5, left). The phase behavior was also predicted using a mean-field thermodynamic model based on a modified theory proposed by Matsuyama for NP−LC mixtures[16] and tailored to the AuNP−5CB system.[17] The extent of particle aggregation and the formation of network structures for different experimental conditions were qualitatively described. This model indicates that the nematic AuNP networks are essentially determined by the phase equilibrium behavior and the nucleation rate of the nematic phase. A phenomenological expression for the mixing interaction parameter was introduced that accounts for entropic and enthalpic effects due to the interaction of the LC host and the ligands in the NP corona. The other details of this model are found in earlier publications.[16−18]

Depending on the nematic order parameter (S) and crystal order parameter (σ) from the particles, four phase behaviors can be predicted from the thermodynamic model: the isotropic (I) phase where $S = \sigma = 0$; the nematic (N) phase where $S > 0$ and $\sigma = 0$; the crystal (C) phase where $S = 0$ and $\sigma > 0$; and the nematic-crystal (NC) phase where $S > 0$ and $\sigma > 0$. In this study, colloidal crystallization was not considered since NMR distinguishes only the nematic versus the isotropic LC and there is no direct measure of the spatial structure of the NPs at the nanoscale. However, as the location of the N + C binodal in this model is very close to the location of N + I binodal, the results would not be significantly affected by including colloidal crystallization. The phase diagrams were constructed in the usual way by equalization of the chemical potentials of each component and minimization of the free energy with respect to the order parameter in each phase. The free energy of the mixture is

$$f = \frac{\phi_{LC}}{\nu_{LC}}\ln(\phi_{LC}) + \frac{\phi_{NP}}{\nu_{NP}}\ln(\phi_{NP}) + \frac{\phi_{NP}}{\nu_{NP}}\frac{4\phi_{NP} - 3\phi_{NP}^{\ 2}}{(1-\phi_{NP})^2} + \chi a_P \phi_{NP}\varphi_{LC} + \frac{\phi_{LC}}{\nu_{LC}}\left[\frac{1}{2}n\varphi_{LC}S^2 - \ln(Z_n)\right] + wS^2 a_P \phi_P \varphi_{LC} \quad (1)$$

The first four terms represent the isotropic mixing free energy where ϕ is the volume fraction and ν is the specific volume. The isotropic binary interaction parameter is $\chi = A + B/T$, where A and B are the enthalpic and entropic contributions that depend strongly on the ligand shell composition and a_P is the particle area per unit volume. $\varphi_{LC} = \phi_{LC}a_{LC}/(\phi_{LC}a_{LC} + \phi_{NP}a_{NP})$ is the area fraction of liquid crystal and represents the probability that the NP surface is in direct contact with a LC molecule. The fifth term is the nematic free energy where S is the scalar nematic order parameter, Z_n the nematic partition function, and $n = 4.54T_{N-I}/T$ is the Maier−Saupe quadrupolar interaction parameter. The last term is due to specific interactions where $w = W/T$ is a binary nematic interaction that accounts for anchoring at the NP surface and distortions in the nematic director at a nanoscale range in the vicinity of a NP. Specific volumes and areas as well as interaction parameters are nondimensionalized with respect to a reference length l_{ref} = 0.53 nm. The parameters A, B, and W are undefined while a_P, a_{LC}, ν_P, and ν_{LC} are geometrical parameters that can be known *a priori*. However, the real value of a_P, which is the "contact area" between a NP corona and a LC molecule, is difficult to estimate since the mixed-ligand corona has free volume and can be penetrated by the solvent. The value calculated from a spherical geometry assumption led to a very poor fitting. The effective contact area is expected to be larger than that corresponding to a hard, perfect sphere. In this perspective, A, B, W, and a_P were considered as adjustable parameters. The parameters ν_P = 1132, ν_{LC} = 3.5, and a_{LC} = 2.57 were calculated as described previously,[17] and the adjustable parameters (and their standard errors) are a_P = 1.16 (0.12), A = 0.823 (0.905), B = −0.106 (0.815), and W = −0.704 (0.012). The parameters A and B are strongly correlated, and their values have a significant statistical uncertainty. All four parameters have a significant effect on the phase diagrams and all are needed to obtain a reasonable fit.

In the case of the more miscible AuNPs, where the orientational order of the 5CB-d_2 matrix was measured as a function of particle concentration (Figure 4), a quantitative phase diagram can be constructed and compared to the model (Figure 5, right). From NMR data, the fraction of isotropic phase in coexistence with the nematic phase, Y, was obtained at several temperatures and compositions, assuming that the amount of each phase is proportional to the height or area of the corresponding NMR peak. This quantity can be calculated from the phase diagram by the lever rule:

$$Y = \frac{\phi - \phi_\alpha}{\phi_\beta - \phi_\alpha} \quad (2)$$

where ϕ is the global composition of the mixture and ϕ_α and ϕ_β are the equilibrium concentrations of the coexisting phases (for nematic−isotropic coexistence α = nematic and β = isotropic). The adjustable parameters were obtained by a least-squares fitting by minimizing the sum of squares of the differences between the experimental and calculated values of Y. A set of experimental values of $Y = 0$ at T = 38 °C was included as, from Figure 4, it can be seen that no isotropic−isotropic equilibrium exists.

In comparing the experimental and theoretical phase diagrams in Figure 5, we note that the fraction of isotropic 5CB (Y) measured for the highest AuNP volume fraction (0.35) is significantly lower than theoretically predicted. Despite this discrepancy, the model and the experiment are in good qualitatively agreement with one another, and there are some interesting conclusions that can be extracted from the values of the fitted parameters: (a) the best fit corresponds to a lower critical codissolution temperature ($B < 0$), which is consistent with the observation that the NP aggregates in the isotropic phase tend to dissolve when the mixture is cooled close to T_{N-I}.[8] (b) The value of the particle area per unit

dx.doi.org/10.1021/la304189n | Langmuir 2013, 29, 1258−1263

volume, a_p = 1.23, is larger than the corresponding value of a hard, perfect sphere (0.3), indicating that the effective contact area is indeed increased by the penetration of LC molecules into the ligand corona. (c) The parameter W = −0.7026, which accounts for anchoring at the AuNP surface and distortions in the nematic director at a nanoscale range in the vicinity of a AuNP, is significantly smaller than zero. This means that the interactions between the AuNPs and LC strongly favor the formation of a nematic phase, although this is not strong enough to overcome the dilution effect. Consequently, the nematic-to-isotropic phase transition temperature decreases when adding AuNPs (Figure S1). In addition, this favorable interaction increases the solubility of the AuNPs in the nematic phase and a relatively broad region of homogeneous nematic phase is observed at low AuNP concentrations.

CONCLUSIONS

In conclusion, the mechanism behind the reversible formation of long-range, periodic nanoparticle structures at the T_{N-I} of the host LC is as follows. Initially, the AuNPs are partially expelled by the orientational order of the growing nematic droplets into the isotropic liquid that becomes progressively enriched in AuNPs. Strong coupling of the AuNP ligands to the LC matrix induces and stabilizes an isotropic−nematic biphasic state. The coexistence of nematic and isotropic liquid, also observed in LC−molecular mixtures, facilitates the diffusion and redistribution of the AuNPs into a spatially regular pattern, resulting in the formation of a quasi-periodic AuNP network rather than a simple bulk phase separation. This molecular-level picture is theoretically confirmed by inputting the NMR data into a mean-field thermodynamic model, generating a phase diagram that displays the biphasic region key to the controllable assembly of gold NPs via the LC phase transition. The topological and geometrical properties of the AuNP assemblies are addressed in a recent publication by a spatiotemporal, nonequilibrium model.[19]

Through our validated thermodynamic modeling, we show that, in contrast to purely elastic-dominated nematic colloids, nematic nanocolloids self-organize through the subtle balance of nanoparticle entropic forces and excluded volume, interface-mediated mesogen and nanoparticle molecular interactions, and couplings between conserved and nonconserved order parameters. Fine-tuning of these interactions through ligand and mesogen chemistry, together with mesoscale modeling, provides a roadmap to achieve new functionalities by merging liquid crystal physics and nanoscience.

ASSOCIATED CONTENT

Supporting Information

Syntheses and characterization of the deuterated ligand and 5CB liquid crystal; DSC study of the dispersions; POM images of AuNPs−LC dispersions in the isotropic and nematic phases; diagram of the isotropic 5CB fraction for the dispersions below T_{N-I}. This material is available free of charge via the Internet at http://pubs.acs.org.

AUTHOR INFORMATION

Corresponding Author

*E-mail: linda.reven@mcgill.ca (L.R.); alejandro.rey@mcgill.ca (A.D.R.).

Notes

The authors declare no competing financial interest.

ACKNOWLEDGMENTS

The authors thank Prof. Robert L. Leheny for the useful discussions. This work is supported by the Fonds quebecois de la recherche sur la nature et les technologies (FQRNT) and the Natural Sciences and Engineering Research Council of Canada (NSERC).

REFERENCES

(1) Stamatoiu, O.; Mirzaei, J.; Feng, X.; Hegmann, T. Nanoparticles in liquid crystals and liquid crystalline nanoparticles. *Top. Curr. Chem.* **2012**, *318*, 331−394.

(2) Shiraishi, Y.; Nishida, N.; Toshima, N. Fabrication of liquid crystal displays containing capped nanoparticles and their electro-optic properties. In *Electrical Phenomena at Interfaces and Biointerfaces: Fundamentals and Applications in Nano-, Bio-, and Environmental Sciences*; Ohshima, H., Ed.; Wiley: NewYork, 2012; pp 373−389.

(3) *Liquid Crystals Beyond Displays: Chemistry, Physics, and Applications*; Li. Q., Ed.; John Wiley & Sons, Inc.: New York, 2012.

(4) Ravnik, M. Colloidal structures in confined nematic liquid crystals. *Liq. Cryst. Today* **2011**, *20*, 77−84.

(5) Bai, Y.; Abbott, N. L. Recent advances in colloidal and interfacial phenomena involving liquid crystals. *Langmuir* **2010**, *27*, 5719−5738.

(6) Skarabot, M.; Musevic, I. Direct observation of interaction of nanoparticles in a nematic liquid crystal. *Soft Matter* **2010**, *6*, 5476−5481.

(7) Tomar, V.; Roberts, T. F.; Abbott, N. L.; Hernández-Ortiz, J. P.; de Pablo, J. J. Liquid crystal mediated interactions between nanoparticles in a nematic phase. *Langmuir* **2012**, *28*, 6124−6131.

(8) Milette, J.; Cowling, S. J.; Toader, V.; Lavigne, C.; Saez, I. M.; Lennox, R. B.; Goodby, J. W.; Reven, L. Reversible long-range network formation in gold nanoparticle - nematic liquid crystal composites. *Soft Matter* **2012**, *8*, 173−179.

(9) Milette, J.; Toader, V.; Reven, L.; Lennox, R. B. Tuning the miscibility of gold nanoparticles dispersed in liquid crystals via the thiol-for-DMAP reaction. *J. Mater. Chem.* **2011**, *21*, 9043−9050.

(10) Meeker, S. P.; Poon, W. C. K.; Crain, J.; Terentjev, E. M. Colloid−liquid-crystal composites: An unusual soft solid. *Phys. Rev. E* **2000**, *61*, R6083.

(11) Beckmann, P. A.; Emsley, J. W.; Luckhurst, G. R.; Turner, D. L. Nuclear spin-lattice relaxation rates in liquid crystals. *Mol. Phys.* **1986**, *59*, 97−125.

(12) Sharma, R.; Taylor, R. E.; Bouchard, L.-S. Intramolecular ligand dynamics in d_{15}-(PPh_3)-capped gold nanoparticles investigated by ^2H NMR. *J. Phys. Chem. C* **2011**, *115* (8), 3297−3303.

(13) Draper, M.; Saez, I. M.; Cowling, S. J.; Gai, P.; Heinrich, B.; Donnio, B.; Guillon, D.; Goodby, J. W. Self-assembly and shape morphology of liquid crystalline gold metamaterials. *Adv. Funct. Mater.* **2011**, *21*, 1260−1278.

(14) Kumar, S.; Pal, S. K. The first examples of terminally thiol-functionalized alkoxycyanobiphenyls. *Liq. Cryst.* **2005**, *32*, 659−661.

(15) Heeks, S. K.; Luckhurst, G. R. Deuterium nuclear magnetic resonance study of the orientational order in the nematic phase of 4-*n*-pentyloxy-4′-cyanobiphenyl. *J. Chem. Soc., Faraday Trans.* **1993**, *89*, 3783−3790.

(16) Matsuyama, A.; Hirashima, R. Phase separations in liquid crystal-colloid mixtures. *J. Chem. Phys.* **2008**, *128*, 044907.

(17) Soulé, E. R.; Milette, J.; Reven, L.; Rey, A. D. Phase equilibrium and structure formation in gold nanoparticles − Nematic liquid crystals composites: experiments and theory. *Soft Matter* **2012**, *8*, 2860−2866.

(18) Soulé, E. R.; Rey, A. D. Modelling complex liquid crystal mixtures: from polymer dispersed mesophase to nematic nanocolloids. *Mol. Simul.* **2012**, *38*, 735−750.

(19) Soulé, E. R.; Lavigne, C.; Reven, L.; Rey, A. D. Multiple interfaces in diffusional interfaces in binary mesogen-nonmesogen mixtures undergoing metastable phase separations. *Phys. Rev. E* **2012**, *86*, 011605.